- Technical Paper -

FIBER BRIDGING EFFECT ON SHEAR BEHAVIOR OF UFC WITH NORMAL CONFINEMENTS

Chikako FUJIYAMA[*1], Kyoichi TOKUTAKE[*2], Yusuke NAGAI[*3] and Yuya TUSJI[*4]

ABSTRACT

The Ultra-high strength Fiber Reinforced Concrete (UFC) subjected to pure shear had been investigated for the specimens with / without steel fibers. The shear capacities were dominated by the confinement stress 5MPa, 10MPa and 15MPa and they were plotted close to the Mohr-Coulomb's failure criterion. The relationship between normal strain to shear strain was classified by existence of fibers rather than confinement stress. The difference of apparent contact angle, assuming equivalent crack opening and equivalent shear slip, for with / without fiber was determined as the fiber bridging effect.

Keywords: UFC, Shear capacity of pre-stressed member, fiber bridging effect, apparent contact angle

1. INTRODUCTION

The Ultra-high strength Fiber Reinforced Concrete, called UFC or UHPFRC had been widely developed in the world for a couple of decades. In order to utilize this high performance material, the constitutive models for compression and tension have been proposed for the structural design.

Currently, the focus has been shifted on the behavior of UFC under the cyclic load. For instance, B. Li *et al.* demonstrated and analyzed experimental investigation of stress-strain behavior based on carefully programmed test series[1]. Further, P. A. Krahl *et al.* proposed a model for damage growth and permanent strains during cyclic compression and installed a function to represent damage evolution[2]. Since tension stiffening is the major advantage of UFC, the studies relating to tension and its modelling are also actively conducted [3) 4)].

The study of shear behavior and shear transfer mechanism of UFC seems not relatively be paid attention from the researchers as compared to the compression and tension[5], since the failure mode of UFC members is basically bending. There is useful research[6] for design for wall and slab, however, the fundamental study under the cyclic shear is limited[7].

Here, this study intends to clarify the fiber bridging effect on shear transfer mechanism of UFC. Specifically, the effect of confinement stresses considering practical use of UFC as pre-stressed concrete members and the contribution ratio of confinement stress and bridging effect is discussed in this paper.

2. TEST PROGRAM

2.1 Materials

(1) Composition of UFC

UFC used in this study consists of cement-based binder, fine aggregate, water and super plasticizer and steel fiber combination of 15mm and 22mm of length with 0.2mm of diameter with the volume ratio 1:1 (0.875vol% : 0.875vol%). The mix proportion is shown in Table 1. Materials were mixed more than 10 minutes, then cured by 85 °C steam for 24 hours after the 24 hours of sealed curing[7]. The fiber bridging effect was examined by the mix which simply removes fiber from the mix on Table 1.

Table 1 Mix proportion

Unit weight kg/m^3				Steel fiber
Water	Binder	Fine aggregate	Super plasticizer	
195	1287	905	32.2	1.75vol.%

(2) Compressive, tensile, and estimated shear strength

The three cylinderical specimens were tested right before the shear test in accordance with JIS A 1108:2006 and JIS A 1149:2010. The results are listed in Table 2. Average compressive strength and Young's modulus were 181 MPa and 43 GPa, respectively.

Table 2 Results of uni-axial compression test

ID	Strength MPa	Strain at peak 10^{-6}	Young's modulus GPa	Poisson's ratio
1	194.41	5108	43.48	0.18
2	176.21	4638	42.39	0.21
3	172.09	4584	43.09	0.20
Average	180.90	4777	42.99	0.20

Bending tensile strength was also examined by

*1 Associate Prof., Dept. of Civil Engineering, Yokohama National University, Dr.E., JCI Member
*2 SHIMIZU CORPORATION, M.E., JCI Member
*3 KAJIMA CORPORATION, M.E., JCI Member
*4 Hanshin Expressway company limited, M.E., JCI Member

JSCE-G552. Average bending tensile strength was 24.23 MPa. According to the guideline [5], a tensile strength of 8.76 MPa can be given by bending tensile strength as follows,

$$f_t = (f_b - 1.54) / 2.59 \quad (1)$$

where,

f_t : tensile strength of UFC (MPa)

f_b : bending tensile strength of UFC (=24.23 MPa)

The shear strength without confinement stress can be also estimated as 19.90 MPa from Mohr's stress circle theory as follows,

$$\tau = (f'_c \times f_t)^{0.5} / 2 + \sigma (f'_c \times f_t) / (2 (f'_c \times f_t)^{0.5}) \quad (2)$$

where,

τ : shear strength (MPa)

σ : confinement strength normal to shear (MPa)

f'_c : uniaxial compressive strength (=180.90 MPa)

2.2 Dimension of specimens

The cross section of specimens are 150 mm of width and 300 mm of height. The total length is 600 mm with the 20 mm height notch on the top and bottom side to induce the dominant shear deformation at the intended cross section as shown in Fig. 1. There are two prestressing steel bars (PC bar) with 32mm of diameter to install confinement stresses. The diameter of Polyethylene (PE) sheath was 38 mm due to eliminate the dowel action from PC bars during shear test.

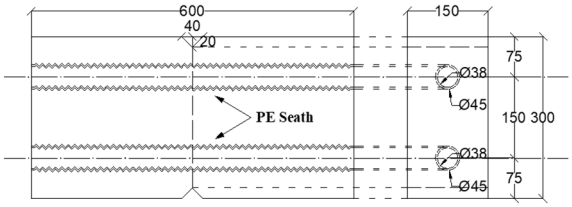

Fig.1 Dimensions of specimen（Unit: mm）

2.3 Loading procedure

The pre-loading provoking a starting point of shear crack surface was conducted as shown in Fig. 2. The splitting load was applied until either the one of the strain gauges comes up to 500 μ or one of the crack displacement transducers comes up to 0.05 mm for the specimens with steel fibers. However, the specimens without steel fiber were sudden split at around 120 μ of strain and around 0.01 mm of crack width. The surfaces of split cracks were almost flat and smooth.

The schematic view of shear test set up is illustrated in Fig. 3. The width of support plates was 40 mm. The confinement stresses were controlled by the hydraulic jacks step by step during the shear loading with tolerance limit ± 0.05 MPa. The static loading-unloading-reloading process was firstly applied for 10 MPa, 20 MPa, 30MPa and 35 MPa of shear stress, then monotonic load was applied until the failure. The all analyses in this study, the shear stress and confinement stress were defined as obtained load divided by the area of notched cross section despite the really formed crack plane shape.

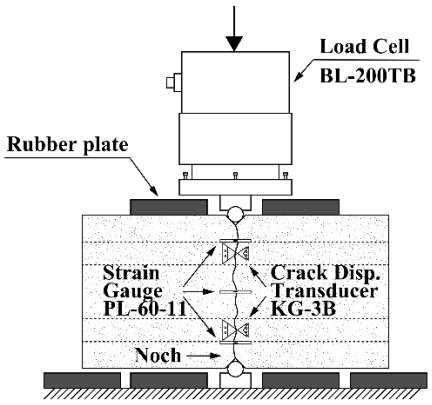

Fig.2 Pre-loading

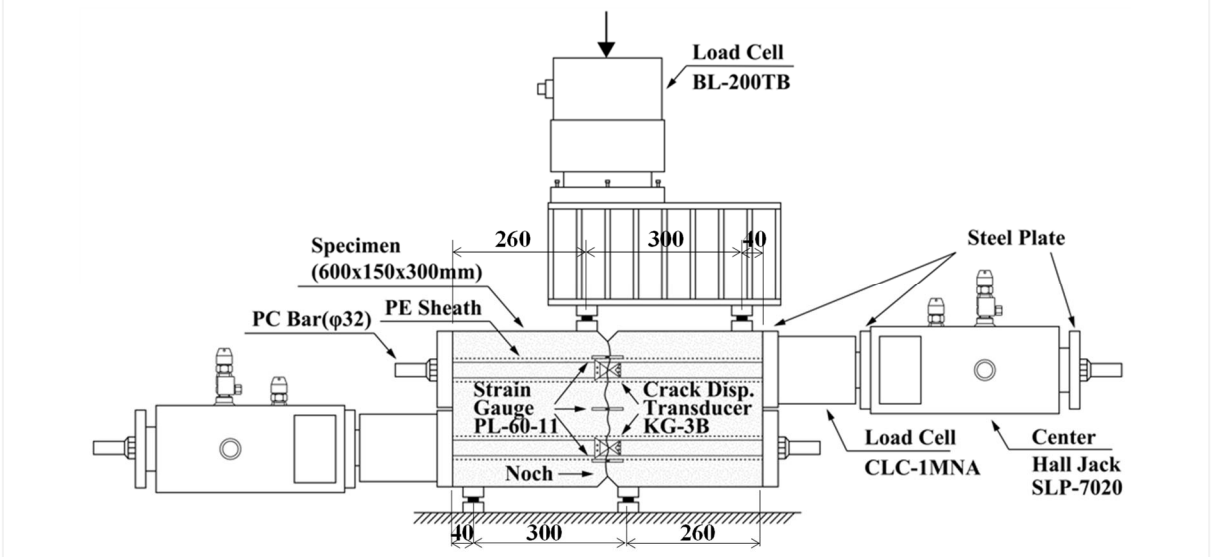

Fig.3 Schematic view of shear test setup from the West side

2.4 Test cases and conditions

The test cases and conditions are summarized in Table 3. The expected shear strengths calculated by equation (2) are shown together. The parameters are existence of fiber and confinement stress. The ID starting from "F" includes fiber and "NF" means the specimen without fiber. The following numbers 5, 10, 15 mean the confinement stresses in MPa unit.

Table 3 Test cases and conditions

ID	Existence of fiber	Confinement stress (MPa)	Expected shear strength (MPa)
F-05-1	✓	5	30.7
F-05-2	✓	5	30.7
F-10-c	✓	10	41.5
F-15-v	✓	10 ->15 ->5	52.3
NF-5	Non	5	---
NF-10	Non	10	---

3. TEST RESULTS AND DISCUSSION

3.1 Shear capacity with confinement

(1) Obtained shear capacity with confinement

The obtained shear strengths in this study are listed together with expected values in Table 4. The obtained strengths were basically higher than the expected ones, even though the pre-loading intending to create split specimen was applied before shear test.

When we compare obtained one and expected one for F series, the excess for 5 MPa was larger than the excess for 10 MPa. Therefore, the effect of confinement stress was not proportional. The shear strengths of NF series were clearly smaller than that of F series. The difference between F series and NF series for 5 MPa and 10 MPa confinement stresses were 27.7 MPa and 24.7 MPa, respectively. These suggest that the shear transferring mechanism of UFC is explained by fiber bridging, and the less contribution of Coulomb's friction.

Table 4 Shear strength

ID	Obtained shear strength (MPa)	Expected shear strength (MPa)	Obtained / expected
F-05-1	35.1	30.7	1.14
F-05-2	39.0	30.7	1.27
F-10-c	42.1	41.5	1.01
F-15-v	44.2	52.3	0.85
NF-5	9.28	---	---
NF-10	17.4	---	---

(2) Verification of test method

Since the relative slips at peak stress obtained from measurement were less than 1 mm, the dowel action should contribute to the shear strength. For this verification, the results in this study were compared with the values obtained by different types of shear test (see Fig. 4 and Fig.5).

The strengths obtained in this study were not obviously larger than others. It is supposed that the dowel action was well eliminated by proper set up. Furthermore, it was found that the shear strengths were almost aligned on the Mohr – Coulomb's criteria despite the difference of shear test method. The intercepts of criteria lines for Nagai *et al* (2021) [6] and this study are 23.3 MPa and 19.9 MPa, respectively. These are close to the standard shear strengths defined by equation (3) in contact density model for ordinally concrete [9] as 23.3 MPa and 21.7 MPa.

$$m = 3.83 f'_c{}^{1/3} \quad (3)$$

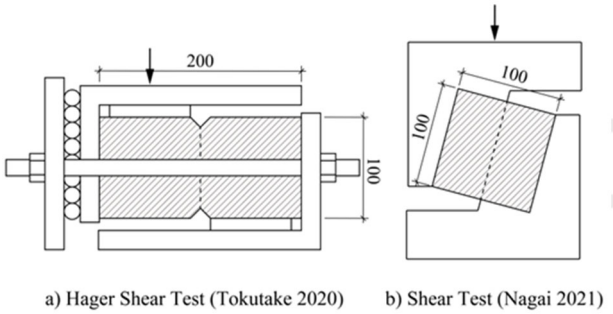

a) Hager Shear Test (Tokutake 2020) b) Shear Test (Nagai 2021)

Fig.4 Shear test method [7) 8)]

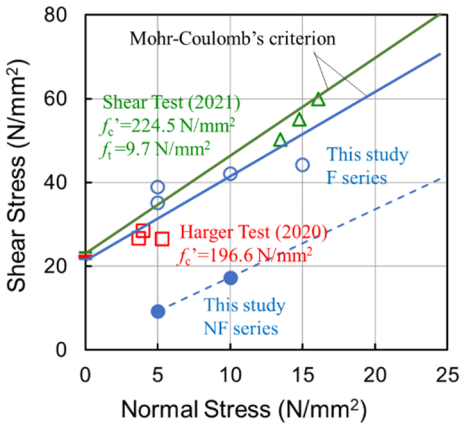

Fig.5 Comparison of shear strengths of UFC obtained by different types of tests [6) 8)]

3.2 Failure modes

(1) F series

The failure modes of F-5-1 and F-15-v are shown in Fig.6. The relative slips of F series were between 0.1 mm and 0.3 mm, however there was no clear trend depending on the confinement stresses. All the specimens in F series didn't show single straight cracks but showed zigzag and diagonal ones. The shapes of observed cracks were different in each side. This is because randomly distributed fibers influenced the surface crack profiles.

(2) NF series

The failure modes of NF-5 and NF-10 are shown in Fig.7. The cracks had been generated by pre-loading and were single and almost straight cracks. Once the confinement stresses applied, these cracks were completely closed and could not be seen by naked eyes. The failure of NF series were sudden and brittle at relative slip less than 0.1 mm.

3.3 Deformation behavior

Since the cracks in F series did not propagate from notch to notch as shown in Fig.8, the constitutive model based on the average stress – average strain relation for smeared crack model was employed here. The relationship between shear stress and the averaged shear strain to the averaged normal strain ratio β[9] were shown

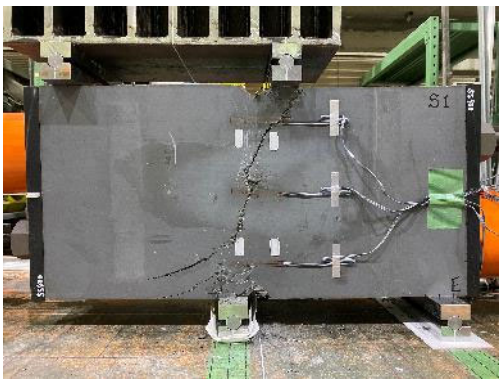

(a) F-5-1 (East side)

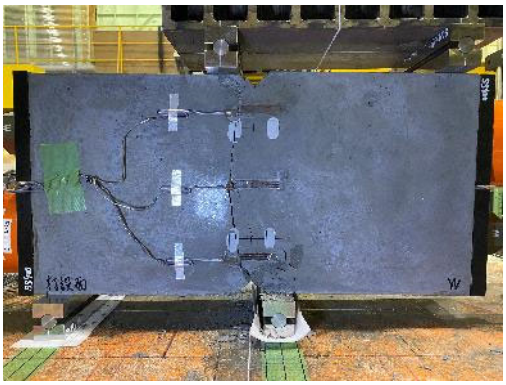

(b) F-5-1 (West side)

(c) F-15-v (East side)

(d) F-15-v (West side)

Fig.6 Failure mode of F-series

(a) NF-5 (East side)

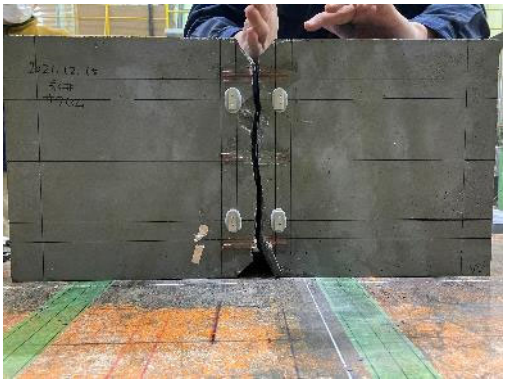

(b) NF-5 (West side)

(c) NF-10 (East side)

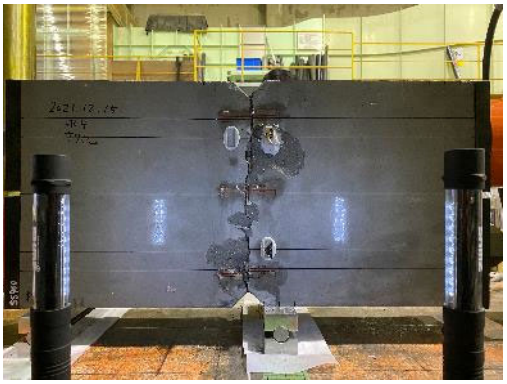

(d) NF-10 (West side)

Fig.7 Failure mode of NF-series

in Fig.8 together with equation (4) proposed for ordinary concrete. Assuming the shear deformed width was 40 mm as the horizontal distance of support plates (see Fig.3), β was calculated from the average measured relative slip and average crack opening.

$$\tau = m\,\beta^2 / (1+\beta^2) \quad (4)$$

where,

m : standard shear strength defined by equation (3)

β : the shear strain to normal strain ratio ($=\gamma_{cr}/\varepsilon_t$)

γ_{cr} : shear strain (=relative slip / 40 mm)

ε_t : normal strain (=crack opening / 40mm)

Note that the Fig. 8 (c) may contain measurement errors because the loosened connectors of displacement transducers were found after the loading. However, we used all data for taking average at this moment due to the difficulty of identifying the timing of loosening.

For the series F, only the loading process was shown. The observed fluctuation was due to the process of adjusting confinement stress. The maximum shear stresses were recorded at less than 1.0 of β, (Fig.8 (a)(b)(d)), even though the trend was not clear for F-10-c (Fig.8 (c)). The inclinations during the loading process were steeper than the line for ordinary concrete. This means that the increment of normal strain accompanied with the development of shear strain was well restrained by confinement stress at the beginning stage as compared to the normal concrete which exhibits the positive dilatancy due to the existence of coarse aggregate. Furthermore, they exhibited somewhat hardening trends right before the maximum records. This suggested that the bond between fiber and binder strongly prevented the failure due to sudden development of shear slip at the last stage. For the series NF, there were no hardening trends, and their envelopes were mild.

3.4 Quantitative analysis of fiber bridging effect

For the quantitative discussion of the fiber bridging effect of UFC in shear, further analysis was needed. The relationship between averaged shear slip

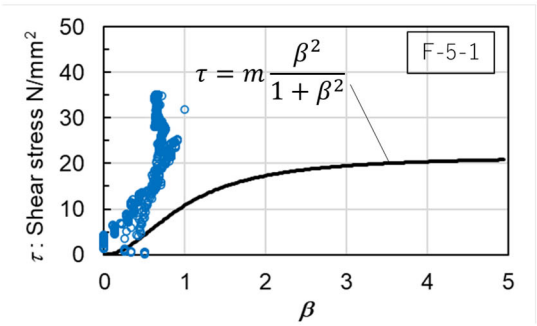

(a) F-05-1 (loading)

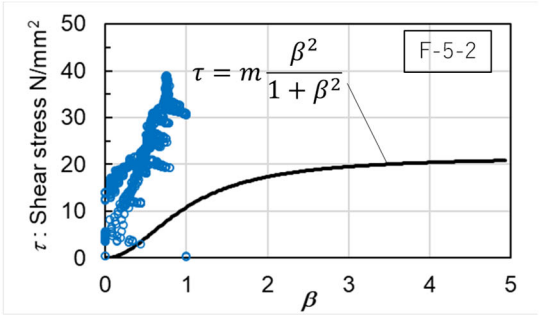

(b) F-05-2 (loading)

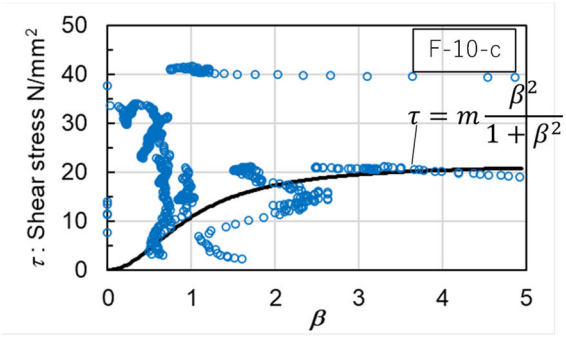

(c) F-10-c (loading)

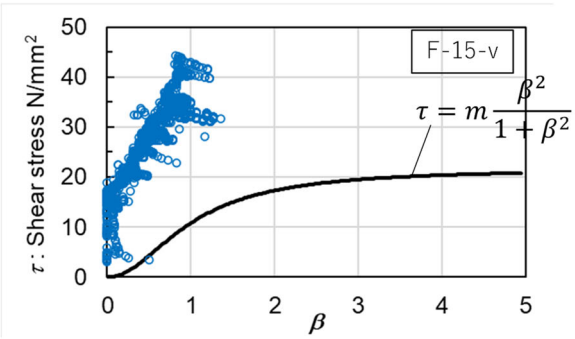

(d) F-15-v (loading)

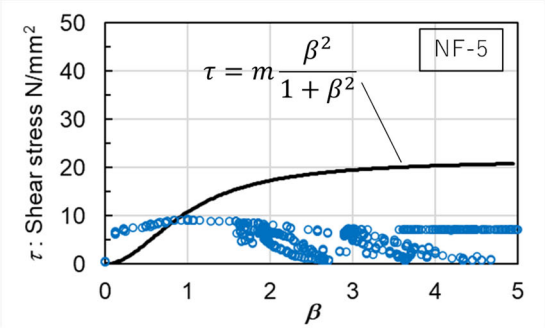

(e) NF-5 (whole history)

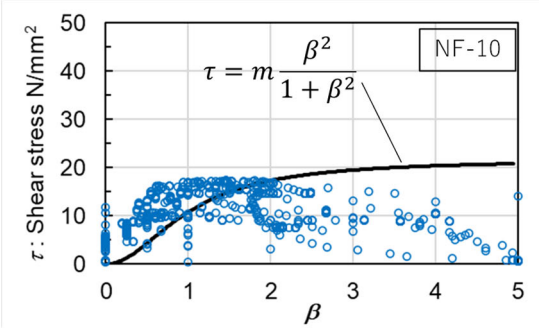

(f) NF-10 (whole history)

Fig.8 Shear stress versus the shear strain to normal strain ratio

and averaged crack opening were directly shown in Fig. 9. The physical meaning of the inclination of lines is simply understood as the apparent contact angle. The case F-10-c was not shown here due to the possibility of errors.

The apparent contact angle for F series ϕ_F was determined as 56 degree in spite of the different confinement stresses. Independence from confinement stress was also observed for NF series. Both NF-5 and NF-10 shows 27 degree which is a half of the F series. The fiber bridging effect was determined as the specific apparent contact angle.

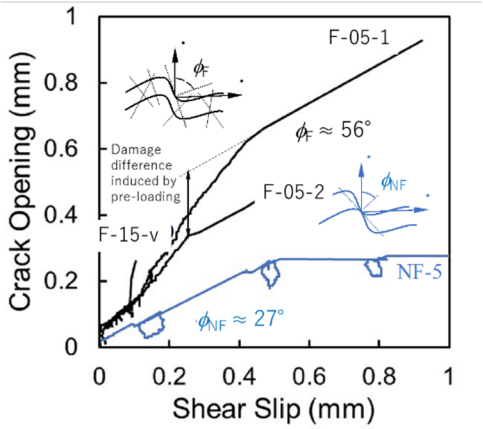

Fig.9 Apparent contact angle

4. CONCLUSIONS

The Ultra-high strength Fiber Reinforced Concrete (UFC) subjected to pure shear had been investigated for the specimens with / without steel fibers under the variation of confinement stress 5MPa, 10MPa and 15MPa. The following conclusions were drawn from the obtained results:

(1) The shear strengths were plotted close to the Mohr-Coulomb's failure criterion, however, the effect of confinement stress was not proportional for the specimens with fiber. This suggests that the shear transferring mechanism of UFC is explained mainly by fiber bridging, and the contribution of Coulomb's friction is relatively small.

(2) The intercepts of criteria lines are close to the standard shear strengths defined in contact density model for ordinally concrete.

(3) There was no clear trend on failure mode depending on the confinement stresses. All the specimens in F series didn't show single straight cracks but showed zigzag and diagonal ones. The shapes of observed cracks were different in each side. This is because the existence of fibers.

(4) On the shear stress versus the shear strain to normal strain ratio, the inclinations during the loading process were steeper than the line for ordinary concrete. Furthermore, they exhibited somewhat hardening trends right before the maximum records. This suggested that the bond between fiber and binder strongly resisted the shear failure.

(5) The apparent contact angle, assuming equivalent crack opening and equivalent shear slip, for F series was determined as 56 degree in spite of the different confinement stresses. That of NF series was 27 degree which is a half of the F series.

ACKNOWLEDGEMENT

The authors are grateful to Prof. K. Maekawa for suggesting the useful data analysis in this paper. A part of this experiment was conducted with Mr. Jorga Kefiyalew Zerfu.

REFERENCES

[1] Biao Li, Lihua Xu, Yin Chi, Biao Huang, Changning Li, Experimental investigation on the stress-strain behavior of steel fiber reinforced concrete subjected to uniaxial cyclic compression, Construction and Building Materials, Volume 140, pp.109-118, 2017

[2] Pablo Augusto Krahl, Gustavo de Miranda Saleme Gidrão, Ricardo Carrazedo, Cyclic behavior of UHPFRC under compression, Cement and Concrete Composites, Volume 104, 103363, 2019

[3] Eduardo J. Mezquida-Alcaraz, Juan Navarro-Gregori, Pedro Serna-Ros, Direct procedure to characterize the tensile constitutive behavior of strain-softening and strain-hardening UHPFRC, Cement and Concrete Composites, Volume 115, 103854, 2021

[4] Jacopo Donnini, Giovanni Lancioni, Gianluca Chiappini, Valeria Corinaldesi, Uniaxial tensile behavior of ultra-high performance fiber-reinforced concrete (uhpfrc): Experiments and modeling, Composite Structures, Volume 258, 113433, 2021

[5] JSCE, guideline of ultra high strength fiber reinforced concrete, concrete library No.113, 2004 [Japanese]

[6] Chung-Chan Hung, Honghao Li, Hong-Chi Chen, High-strength steel reinforced squat UHPFRC shear walls: Cyclic behavior and design implications, Engineering Structures, Volume 141, pp.59-74, 2017

[7] Nagai Y., Ichimiya T. Kosaka T. and Hamasaki K., Influence of cyclic load on the mechanical properties of UFC, Proceedings of JCI, Vol.43, No.1, pp.203-208, 2021 [Japanese]

[8] Tokutake K. and Fujiyama C. Shear transfer mechanism of UFC subjected to cyclic load, Proceedings of 75th annual conference of JSCE, V-646, 2020 [Japanese]

[9] Baolu Li, Koichi Maekawa and Hajime Okamura, Contact density model for stress transfer across cracks in concrete, Journal of the faculty of engineering, the university of Tokyo (B), Vol. XXXX, No.1, pp. 9-51, 1989